Published in final edited form as:

Cell Rep. 2018 May 01; 23(5): 1249–1258. doi:10.1016/j.celrep.2018.03.132.

ZNF598 Plays Distinct Roles in Interferon-Stimulated Gene Expression and Poxvirus Protein Synthesis

Stephen DiGiuseppe[1], **Madeline G. Rollins**[1], **Elizabeth T. Bartom**[2], and **Derek Walsh**[1,3,*]

[1]Department of Microbiology-Immunology, Feinberg School of Medicine, Northwestern University, Chicago, IL 60611, USA

[2]Department of Biochemistry and Molecular Genetics, Feinberg School of Medicine, Northwestern University, Chicago, IL 60611, USA

SUMMARY

Post-translational modification of ribosomal subunit proteins (RPs) is emerging as an important means of regulating gene expression. Recently, regulatory ubiquitination of small RPs RPS10 and RPS20 by the ubiquitin ligase ZNF598 was found to function in ribosome sensing and stalling on internally polyadenylated mRNAs during ribosome quality control (RQC). Here, we reveal that ZNF598 and RPS10 negatively regulate interferon-stimulated gene (ISG) expression in primary cells, depletion of which induced ISG expression and a broad antiviral state. However, cell lines lacking interferon responses revealed that ZNF598 E3 ligase activity and ubiquitination of RPS20, but not RPS10, were specifically required for poxvirus replication and synthesis of poxvirus proteins whose encoding mRNAs contain unusual 5′ poly(A) leaders. Our findings reveal distinct functions for ZNF598 and its downstream RPS targets, one that negatively regulates ISG expression and infection by a range of viruses while the other is positively exploited by poxviruses.

In Brief

In addition to repressing poly(A) readthrough during ribosome quality control, DiGiuseppe et al. report that ZNF598 and RPS10 negatively regulate interferon-stimulated gene expression (ISG). However, in cell lines lacking ISG responses, ZNF598 ubiquitin ligase activity and RPS20 ubiquitination are specifically required by poxviruses, which produce unusual mRNAs with 5′ poly(A) leaders.

*Correspondence: derek.walsh@northwestern.edu.
[3]Lead Contact

SUPPLEMENTAL INFORMATION

Supplemental Information includes Supplemental Experimental Procedures and two tables and can be found with this article online at https://doi.org/10.1016/j.celrep.2018.03.132.

AUTHOR CONTRIBUTIONS

S.D. and M.G.R. designed and conducted experiments and analyzed data. E.T.B. performed codon analysis. D.W. conceived the project, designed experiments, analyzed data, and wrote the manuscript. All authors contributed to editing the manuscript.

DECLARATION OF INTERESTS

The authors declare no competing interests.

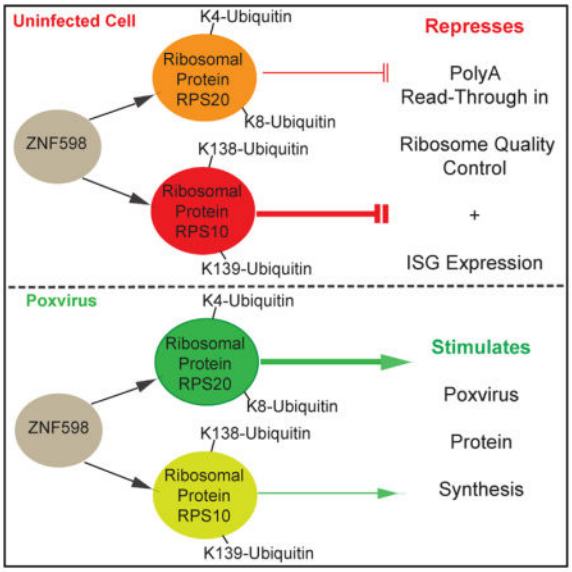

INTRODUCTION

While ribosomes are often viewed as indiscriminate, evidence is emerging that they have the ability to selectively control translation. This discriminatory capacity arises from changes in the composition of or post-translational modifications (PTMs) to RPs. Evidence for this comes from cell-type-specific expression of the large RP, RPL38, that selectively regulates translation of Homeobox (HOX) mRNAs during developmental patterning (Kondrashov et al., 2011; Xue et al., 2015), as well as likely subunit heterogeneity within the subcellular pool of ribosomes (Shi et al., 2017). However, while many PTMs to ribosomal proteins have been identified, few have been found to have regulatory functions on the ribosome that control translational specificity (Simsek and Barna, 2017).

Recently, regulatory ubiquitination of small RPs (RPSs) was found to promote stress survival (Higgins et al., 2015; Silva et al., 2015) and also functions in ribosome quality control (RQC). RQC involves the recognition of aberrant mRNAs or translation events that cause ribosomes to stall, leading to mRNA and nascent peptide chain destruction together with recycling of stalled ribosomes back into the active pool. While the factors that direct these terminal events are well characterized (Joazeiro, 2017), recent work has begun to reveal how ribosome stalls occur and are sensed, which involves regulatory rather than proteasome-targeting ubiquitination events.

Yeast and mammals use related factors in early RQC but there are fundamental differences in how they operate. In yeast, the poly-basic peptides encoded by consecutive CGA (arginine) or AAA/AAG (lysine) codons are potent inducers of ribosome stalling (Letzring et al., 2013; Lu and Deutsch, 2008). However, homopolymeric adenosine (poly(A)) tracts are particularly potent in mammals. This is because beyond the stall-inducing lysine chains they encode, the poly(A) sequence itself causes frame-shifts irrespective of whether they are in frame to code for lysines (Arthur et al., 2015). Frameshifts occur because poly(A) tracts ≥11 nt cause bidirectional ribosome sliding and are heavily selected against in coding

regions (Arthur et al., 2015; Koutmou et al., 2015; Shirokikh and Spirin, 2008). However, more complete ribosome stalling that prevents eventual readthrough seems to require longer poly(A) lengths (Juszkiewicz and Hegde, 2017). For this reason, the long 3′ poly(A) tails on mammalian mRNAs act as sentinels for aberrant transcripts or translational events. Decoding of the poly(A) tail arising from frameshifts or on mRNAs lacking a stop codon stalls ribosomes resulting in non-stop decay (NSD), while premature polyadenylation in coding regions causes No-Go Decay (NGD) (Joazeiro, 2017). This specific sentinel function of the poly(A) tail may have evolved in the face of more complex and error-prone mRNA biogenesis pathways in mammals, as their poly(A) tails are longer than in plants or fungi (Subtelny et al., 2014; Tian and Manley, 2013).

Recent work has also begun to identify the proteins involved in initiating RQC, which also exhibit functional differences between yeast and mammals. These include Asc1 (Receptor for Activated C kinase 1 [RACK1] in mammals), RPL1, and the ubiquitin ligase HEL2 (ZNF598 in mammals) (Garzia et al., 2017; Juszkiewicz and Hegde, 2017; Letzring et al., 2013; Saito et al., 2015; Simms et al., 2017; Sitron et al., 2017; Sundaramoorthy et al., 2017). In yeast, Asc1 and HEL2 function in nascent chain modification and degradation but are not required for ribosome arrest at stall sequences or for NSD, perhaps because of shorter yeast poly(A) tails (Saito et al., 2015; Sitron et al., 2017). By contrast, in mammals ZNF598 binds ribosomes, mRNA, and Lys^{UUU}-tRNAs and acts as a sensor for poly(A) (Garzia et al., 2017; Juszkiewicz and Hegde, 2017; Simms et al., 2017; Sundaramoorthy et al., 2017). Upon encountering stall-inducing poly(A) sequences, ZNF598 induces site-specific ubiquitination of RPS10, RPS20, and RPS3 (Garzia et al., 2017; Juszkiewicz and Hegde, 2017; Simms et al., 2017; Sundaramoorthy et al., 2017). In the absence of ZNF598 E3 ligase activity or in cells with ubiquitin-site mutations in RPSs, particularly RPS10, ribosomes read through poly(A) and RQC is not induced. While Asc1/RACK1 contribute to stalling and nascent chain destruction (Gandin et al., 2013; Ikeuchi and Inada, 2016; Kuroha et al., 2010; Matsuda et al., 2014; Sitron et al., 2017), in mammals RACK1 can also influence RPS ubiquitination despite the fact it has no known ubiquitin ligase activity (Sundaramoorthy et al., 2017).

We recently showed that the poxvirus, Vaccinia Virus (VacV) causes unique phosphorylation events in RACK1 to enhance translation of its mRNAs that contain unusual 5′ leaders consisting almost exclusively of poly(A) (Jha et al., 2017; Walsh, 2017). This prompted us to test whether poxviruses might also utilize ZNF598 and RPS ubiquitination.

RESULTS

To test whether ZNF598 functioned in poxvirus infection, we first depleted ZNF598 in primary normal human dermal fibro-blasts (NHDFs). Western blot (WB) analysis showed that NHDFs express low levels of ZNF598 that migrates as a doublet, similar to HCT116 cells previously used to study ZNF598 (Sundaramoorthy et al., 2017) (Figure 1A). Moreover, ZNF598 was efficiently depleted in NHDFs by two independent small interfering RNAs (siRNAs). To test effects of ZNF598 depletion on virus spread, siRNA-treated NHDFs were infected at low multiplicity of infection (MOI) with VacV expressing a GFP-tagged viral protein, B5. Imaging and quantification showed that in control siRNA-treated

cultures, VacV-B5-GFP spread to form plaques, but spread in ZNF598-depleted cultures was significantly impaired (Figures 1B and 1C). However, ZNF598 depletion also suppressed the spread of an unrelated DNA virus, herpes simplex virus type 1 (HSV-1) expressing a GFP-tagged viral protein, Us11 (Figures 1B and 1C). To test this further, we infected control and ZNF598-depleted NHDFs at high MOI and assessed effects on viral protein synthesis in single round infections, expanding to include the RNA virus, vesicular stomatitis virus (VSV). ^{35}S metabolic labeling showed that each virus suppressed host translation and produced a characteristic pattern of viral proteins in control siRNA-treated cells (Figure 1D). However, both ZNF598 siRNAs suppressed viral protein synthesis and sustained host translation, suggesting a block to infection by all three viruses. Verifying this, WB analysis showed that ZNF598 depletion reduced the accumulation of VacV, HSV-1, or VSV antigens in infected cells (Figures 1E–1G). Moreover, WB analysis revealed that while β-actin was relatively unaffected, interferon-inducible proteins ISG56, PKR, and MxA were greatly elevated in ZNF598-depleted NHDFs (Figures 1E–1G). This also occurred in uninfected cells, demonstrating that this was not in response to infection but that ZNF598 generally repressed interferon-stimulated gene (ISG) expression. While analysis of human codon sequences showed that the specific ISGs examined did not contain poly(A) tracts >7 nt (Table S1), prior analyses of this kind identified significant enrichment of nucleotide and nucleic acid binding proteins that conceivably regulate their induction (Arthur et al., 2015). We also noted enrichment of transcripts belonging to the killer immunoglobulin-like receptor (KIR) cluster (Table S1). This suggests that open reading frames (ORFs) encoding proteins involved in antiviral responses contain poly(A) tracts, which may explain their repression by ZNF598.

The induction of an antiviral state in NHDFs confounded our goal of determining whether poxviruses utilize ZNF598. To circumvent this, we noted that many transformed cell lines are defective in interferon signaling. Therefore, we examined infection in a human colon epithelial line, HCT116 for which previously characterized CRISPR-derived ZNF598 knockout (KO) and rescue lines were available (Sundaramoorthy et al., 2017). Initial low MOI spreading assays using VacV-B5-GFP or HSV-1-GFP-Us11 revealed that VacV spread was suppressed in ZNF598-KO cells compared with parental cells (Figures 2A and 2B). Moreover, VacV spread was restored in ZNF598-KO cells rescued with WT ZNF598, but only partially rescued by ZNF598-C29A, a mutant with reduced ubiquitin ligase activity (Sundaramoorthy et al., 2017). By contrast, HSV-1 formed plaques in all four HCT116 lines independently of ZNF598 or its ligase activity. To examine this in more detail, HCT116 lines were infected at high MOI with VacV, HSV-1, or VSV. WB analysis confirmed that ZNF598 KO did not increase ISG expression in either uninfected or infected HCT116 cells (Figures 2C–2F). In the absence of ISG induction, both HSV-1 and VSV antigens accumulated at comparable levels in all four HCT116 lines (Figures 2C and 2D). By contrast, both the production of infectious virus and the accumulation of intermediate (I3) or late (D8 and A14) poxvirus proteins was impaired in ZNF-KO cells; this was rescued by expression WT ZNF598 but was only partially rescued by ligase-impaired ZNF598-C29A (Figures 2E and 2F). PCR analysis showed that this was not due to defects in the production of the mRNA encoding each poxvirus protein (Figure 2G). Notably, reductions in protein levels for the late protein, A14, appeared larger than for the intermediate protein, I3 (Figure 2F). This was in

line with our broader understanding of poxvirus biology; intermediate proteins such as I3 accumulate during early-intermediate stages of infection. However, their synthesis is further enhanced during the transition to late stages when the virus extensively remodels the host translation system to favor viral mRNAs with poly(A) leaders (Dhungel et al., 2017; Jha et al., 2017). Late mRNAs made at the time of this transition therefore suffer most when the process is impaired, and our data suggest that ZNF598 is an important component of this transition.

Genome analysis revealed that 57% of poxvirus ORFs harbor at least one adenosine homopolymer ≥6 nt compared with 23.3% in human ORFs (Tables S1 and S2). However, these poly(A) runs were found in early, intermediate, and late viral genes. Moreover, in contrast to their randomly generated leaders ranging 12–50 nt (Walsh, 2017), all viral ORFs contained poly(A) tracts below the 11nt limit for ribosome sliding. This suggests that poxvirus ORFs would not be subjected sliding or RQC-mediated repression. Indeed, if this were the case ZNF598 KO would be predicted to enhance rather than repress poxvirus translation, as it does for poly(A) readthrough in RQC and ISG expression, above.

To explore this further, we examined whether VacV infection altered RPS ubiquitination in a ZNF598-dependent manner. ZNF598 is required for RPS10 ubiquitination and stimulates RPS20 ubiquitination (Garzia et al., 2017; Juszkiewicz and Hegde, 2017; Sundaramoorthy et al., 2017). Similarly, although VacV did not stimulate the ubiquitination of either RPS10 or RPS20 above that of uninfected HCT116 cells, ubiquitination of these proteins remained dependent on ZNF598 E3 ligase activity (Figure 3A). This suggested that VacV did not activate RQC pathways but potentially exploited them in other ways. To test this, we next examined the contribution of RPS substrates of ZNF598 to infection, beginning with primary cells. NHDFs were treated with control or RPS-targeting siRNAs followed by infection at high MOI. WB analysis showed that depletion of RPS10 modestly suppressed production of VacV late proteins, D8 and A14, but had no effect on HSV-1 protein levels (Figures 3B and 3C). However, RPS10 depletion also increased the expression of ISG56 and PKR in both uninfected and infected cells, albeit not to the extent observed with ZNF598 depletion that potently blocked infection by both viruses (Figures 1E and 1F). Different viruses have different sensitivity thresholds to interferon, and weaker effects on HSV-1 would become cumulative and detectable over multiple rounds of replication. In line with this, when RPS10-depleted NHDFs were infected at low MOI for several days defects in the spread of both viruses became evident (Figure 3D). Overall, these findings showed that VacV was more dependent on RPS10 than HSV-1, but that these effects were likely in part due to ISG induction. Moreover, the more modest effects on ISG levels and infection suggested that RPS10 is one of what are likely a number of substrates that enable ZNF598 to control the antiviral state.

By contrast, depletion of RPS20 did not induce ISG expression in uninfected NHDFs and modestly suppressed ISG levels in NHDFs infected with HSV-1 or VSV, but not VacV (Figures 3E–3G). Despite this reduction in ISG levels, RPS20 depletion had no effect on the production of viral proteins by HSV-1 or VSV (Figures 3E and 3F), the latter being extremely sensitive to interferon. This suggests that RPS20 may modestly stimulate ISG production in response to specific viruses, but that neither HSV-1 nor VSV require high

levels of RPS20 to synthesize their own proteins. By contrast, despite having no impact on ISG expression during poxvirus infection depletion of RPS20 reduced VacV protein levels, the extent of which correlated with the degree of RPS20 depletion (Figure 3G). Overall, this suggested that RPS20 was specifically required for poxvirus protein production.

To avoid the influence of interferon responses and test whether RPS ubiquitination functioned in infection, we next examined the replication and spread of VacV or VSV in 293 cells expressing wild-type or ubiquitin-site mutants of RPS10 or RPS20 (Juszkiewicz and Hegde, 2017). WB analysis showed that expression of RPS10 or RPS20 site mutants did not induce ISG expression in these cell lines (Figures 4A–4D). Infection assays revealed that lysine-arginine mutations at either the K138 or K138/K139 ubiquitination sites in RPS10 that are targeted by ZNF598 had no discernible effect on the spread of either VacV or VSV (Figures 4A and 4B). By contrast, mutations at either lysines K8 or K4/K8 of RPS20 potently suppressed VacV spread and protein accumulation (Figure 4C), but had no effect on VSV infection (Figure 4D). It must be noted that the level of RPS10 overexpression in these cells was lower than that of RPS20. This may influence how effectively RPS10 can function as a dominant negative, although in the exact same cell system RPS10 mutants regulate RQC more effectively than RPS20 mutants (Juszkiewicz and Hegde, 2017). In addition, our data in these 293 cells are in line with effects of RPS10 versus RPS20 depletion in NHDFs, above. As such, our cumulative data in different cell systems support the notion that poxviruses specifically exploit ZNF598 and RPS20 ubiquitination, and to a lesser extent RPS10 for their replication.

DISCUSSION

Our findings reveal distinct functions for ZNF598 in regulating host ISG expression and poxvirus protein synthesis (Figure 4E). We provide evidence that ZNF598 and its substrate RPS10 suppress ISG expression, mirroring the factor requirements to suppress poly(A) readthrough in RQC (Garzia et al., 2017; Juszkiewicz and Hegde, 2017; Sundaramoorthy et al., 2017). While it requires further testing, the presence of poly(A) tracts in ORFs of KIR genes as well as transcription factors that potentially serve as broader regulators of ISG expression (Arthur et al., 2015) raises the intriguing possibility that ZNF598 can also suppress readthrough or sliding on shorter poly(A) tracts that influence translational efficiency (Arthur et al., 2015; Koutmou et al., 2015).

Perhaps most surprising is the stimulatory role that ZNF598 plays in poxvirus translation, which also suggests a role for ZNF598 during scanning. Although limited studies of ZNF598 to date have focused on its role in 80S stalling, its primary substrates are RPSs and a large fraction of the cellular pool of ZNF598 co-sediments with initiation factors and 40S subunits (Garzia et al., 2017; Sundaramoorthy et al., 2017). As such, roles in scanning are very plausible, at least in contexts where poly(A) is present in 5′ UTRs. Indeed, evidence suggests that ZNF598 senses poly(A) (Garzia et al., 2017) but precisely how it does so remains unclear. However, this may be specific to poxviruses as poly(A) leaders are not naturally present and do not naturally function as enhancers in mammals (Walsh, 2017). Indeed, poxviruses extensively remodel the host cell to enable poly(A) leaders to function (Dhungel et al., 2017; Jha et al., 2017). Poxviruses induce unique modifications to several

ribosomal proteins (Beaud et al., 1989), including phosphorylation of RACK1 at sites that mimic the negatively charged state of RACK1 in plants, where poly(A) leaders naturally act as enhancers (Jha et al., 2017). While VacV only modestly altered RPS10 and RPS20 ubiquitination levels, suggesting it passively exploits ZNF598 activity, we cannot rule out the possibility that poxviruses repurpose ZNF598 in some way to render it a stimulatory rather than repressive factor.

Despite these differences, there are some intriguing parallels between how poxviruses control their translation and how RQC operates in uninfected cells. RQC is activated on poly(A) but not polyU, and readthrough repression depends more on RPS10 than RPS20 ubiquitination (Garzia et al., 2017; Juszkiewicz and Hegde, 2017; Simms et al., 2017; Sundaramoorthy et al., 2017). Conversely, poxviruses stimulate translation from poly(A) but not polyU leaders (Jha et al., 2017), and as we show here they depend more on RPS20 than RPS10 ubiquitination. RQC was recently found to be activated by ribosome collisions on stall elements, and factors that slow ribosome “traffic,” manifested as reduced polysome levels, enable readthrough (Letzring et al., 2013; Simms et al., 2017). Poxvirus-modified RACK1 causes similar effects on polysomes, suggesting this offsets sliding to enhance poxvirus translation (Jha et al., 2017). Indeed, RACK1 can regulate frameshifting and readthrough of stall sequences (Gandin et al., 2013; Ikeuchi and Inada, 2016; Kuroha et al., 2010; Matsuda et al., 2014; Sitron et al., 2017; Sundaramoorthy et al., 2017; Wolf and Grayhack, 2015). Thus, beyond phosphorylating RACK1 poxviruses appear to co-opt a wider range of factors involved in their mammalian host’s poly(A)-based RQC system but turns them on their head to stimulate viral protein synthesis. Future studies of how ZNF598 has opposing effects on ISG expression and poxvirus protein synthesis will provide important insights into the functions of ribosomal PTMs and translational specification.

EXPERIMENTAL PROCEDURES

Further details and an outline of resources used in this work can be found in Supplemental Experimental Procedures.

Infection Assays

NHDF, HEK293, or HCT116 cells were infected at the indicated MOI with the indicated viruses for the indicated times. Cultures were then imaged using a Leica DMI6000B-AFC wide-field microscope to assess plaque sizes, lysed in Laemmli buffer to perform WB analysis of viral or host protein levels, or freeze-thawed to assess viral titers. Viral titers were measured by serial dilution and plating on permissive BSC40 cells.

RT-PCR Analysis

Total RNA was isolated using Trizol and reverse transcribed using Transcriptor First cDNA synthesis kits. PCR was performed using the primers detailed in the Resource Table in the Supplemental Experimental Procedures.

Analysis of poly(A) Tracts

Poxvirus cDNA sequences were extracted from the Vaccinia virus, Western Reserve genome AY243312.1 at GenBank. Human cDNA sequences were downloaded through Ensembl's Biomart service, version 89. cDNA sequences were filtered for duplicates and analyzed using a perl script to identify poly(A) runs ≥6 nt.

Statistical Analysis

Statistical analysis was performed using GraphPad Prism 6.01. Significance was determined using Student's t test.

Supplementary Material

Refer to Web version on PubMed Central for supplementary material.

Acknowledgments

We thank Eric Bennett, Ramanujan Hegde, Ian Mohr, Paula Traktman, Bernard Moss, and Yan Xiang for reagents. We thank Eric Bennett for fruitful discussions that helped conceive this project. This work was supported by grants from the NIH (R01AI127456 to D.W. and R50CA221848 to E.T.B.). S.D. was supported by training grant T32 AI0007476. M.G.R. was supported by training grant T32 GM008061.

References

Arthur, L., Pavlovic-Djuranovic, S., Smith-Koutmou, K., Green, R., Szczesny, P., Djuranovic, S. Translational control by lysine-encoding A-rich sequences. Sci Adv. 2015. Published online July 1, 2015. https://doi.org/10.1126/sciadv.1500154

Beaud G, Masse T, Madjar JJ, Leader DP. Identification of induced protein kinase activities specific for the ribosomal proteins uniquely phosphorylated during infection of HeLa cells with vaccinia virus. FEBS Lett. 1989; 259:10–14. [PubMed: 2599098]

Dhungel P, Cao S, Yang Z. The 5′-poly(A) leader of poxvirus mRNA confers a translational advantage that can be achieved in cells with impaired cap-dependent translation. PLoS Pathog. 2017; 13:e1006602. [PubMed: 28854224]

Gandin V, Gutierrez GJ, Brill LM, Varsano T, Feng Y, Aza-Blanc P, Au Q, McLaughlan S, Ferreira TA, Alain T, et al. Degradation of newly synthesized polypeptides by ribosome-associated RACK1/c-Jun N-terminal kinase/eukaryotic elongation factor 1A2 complex. Mol Cell Biol. 2013; 33:2510–2526. [PubMed: 23608534]

Garzia A, Jafarnejad SM, Meyer C, Chapat C, Gogakos T, Morozov P, Amiri M, Shapiro M, Molina H, Tuschl T, Sonenberg N. The E3 ubiquitin ligase and RNA-binding protein ZNF598 orchestrates ribosome quality control of premature polyadenylated mRNAs. Nat Commun. 2017; 8:16056. [PubMed: 28685749]

Higgins R, Gendron JM, Rising L, Mak R, Webb K, Kaiser SE, Zuzow N, Riviere P, Yang B, Fenech E, et al. The unfolded protein response triggers site-specific regulatory ubiquitylation of 40S ribosomal proteins. Mol Cell. 2015; 59:35–49. [PubMed: 26051182]

Ikeuchi K, Inada T. Ribosome-associated Asc1/RACK1 is required for endonucleolytic cleavage induced by stalled ribosome at the 3′ end of nonstop mRNA. Sci Rep. 2016; 6:28234. [PubMed: 27312062]

Jha S, Rollins MG, Fuchs G, Procter DJ, Hall EA, Cozzolino K, Sarnow P, Savas JN, Walsh D. Trans-kingdom mimicry underlies ribosome customization by a poxvirus kinase. Nature. 2017; 546:651–655. [PubMed: 28636603]

Joazeiro CAP. Ribosomal stalling during translation: Providing substrates for ribosome-associated protein quality control. Annu Rev Cell Dev Biol. 2017; 33:343–368. [PubMed: 28715909]

Juszkiewicz S, Hegde RS. Initiation of quality control during poly(A) translation requires site-specific ribosome ubiquitination. Mol Cell. 2017; 65:743–750. [PubMed: 28065601]

Kondrashov N, Pusic A, Stumpf CR, Shimizu K, Hsieh AC, Ishijima J, Shiroishi T, Barna M. Ribosome-mediated specificity in Hox mRNA translation and vertebrate tissue patterning. Cell. 2011; 145:383–397. [PubMed: 21529712]

Koutmou KS, Schuller AP, Brunelle JL, Radhakrishnan A, Djuranovic S, Green R. Ribosomes slide on lysine-encoding homopolymeric A stretches. eLife. 2015; 4 Published online February 19, 2015. https://doi.org/10.7554/eLife.05534.

Kuroha K, Akamatsu M, Dimitrova L, Ito T, Kato Y, Shirahige K, Inada T. Receptor for activated C kinase 1 stimulates nascent polypeptide-dependent translation arrest. EMBO Rep. 2010; 11:956–961. [PubMed: 21072063]

Letzring DP, Wolf AS, Brule CE, Grayhack EJ. Translation of CGA codon repeats in yeast involves quality control components and ribosomal protein L1. RNA. 2013; 19:1208–1217. [PubMed: 23825054]

Lu J, Deutsch C. Electrostatics in the ribosomal tunnel modulate chain elongation rates. J Mol Biol. 2008; 384:73–86. [PubMed: 18822297]

Matsuda R, Ikeuchi K, Nomura S, Inada T. Protein quality control systems associated with no-go and nonstop mRNA surveillance in yeast. Genes Cells. 2014; 19:1–12. [PubMed: 24261871]

Saito K, Horikawa W, Ito K. Inhibiting K63 polyubiquitination abolishes no-go type stalled translation surveillance in Saccharomyces cerevisiae. PLoS Genet. 2015; 11:e1005197. [PubMed: 25909477]

Shi Z, Fujii K, Kovary KM, Genuth NR, Rost HL, Teruel MN, Barna M. Heterogeneous ribosomes preferentially translate distinct subpools of mRNAs genome-wide. Mol Cell. 2017; 67:71–83. [PubMed: 28625553]

Shirokikh NE, Spirin AS. Poly(A) leader of eukaryotic mRNA bypasses the dependence of translation on initiation factors. Proc Natl Acad Sci USA. 2008; 105:10738–10743. [PubMed: 18658239]

Silva GM, Finley D, Vogel C. K63 polyubiquitination is a new modulator of the oxidative stress response. Nat Struct Mol Biol. 2015; 22:116–123. [PubMed: 25622294]

Simms CL, Yan LL, Zaher HS. Ribosome collision is critical for quality control during no-go decay. Mol Cell. 2017; 68:361–373. [PubMed: 28943311]

Simsek D, Barna M. An emerging role for the ribosome as a nexus for post-translational modifications. Curr Opin Cell Biol. 2017; 45:92–101. [PubMed: 28445788]

Sitron CS, Park JH, Brandman O. Asc1, Hel2, and Slh1 couple translation arrest to nascent chain degradation. RNA. 2017; 23:798–810. [PubMed: 28223409]

Subtelny AO, Eichhorn SW, Chen GR, Sive H, Bartel DP. Poly(A)-tail profiling reveals an embryonic switch in translational control. Nature. 2014; 508:66–71. [PubMed: 24476825]

Sundaramoorthy E, Leonard M, Mak R, Liao J, Fulzele A, Bennett EJ. ZNF598 and RACK1 regulate mammalian ribosome-associated quality control function by mediating regulatory 40S ribosomal ubiquitylation. Mol Cell. 2017; 65:751–760. [PubMed: 28132843]

Tian B, Manley JL. Alternative cleavage and polyadenylation: The long and short of it. Trends Biochem Sci. 2013; 38:312–320. [PubMed: 23632313]

Walsh D. Poxviruses: Slipping and sliding through transcription and translation. PLoS Pathog. 2017; 13:e1006634. [PubMed: 29145493]

Wolf AS, Grayhack EJ. Asc1, homolog of human RACK1, prevents frameshifting in yeast by ribosomes stalled at CGA codon repeats. RNA. 2015; 21:935–945. [PubMed: 25792604]

Xue S, Tian S, Fujii K, Kladwang W, Das R, Barna M. RNA regulons in Hox 5′ UTRs confer ribosome specificity to gene regulation. Nature. 2015; 517:33–38. [PubMed: 25409156]

Highlights

- ZNF598 negatively regulates interferon-stimulated gene (ISG) expression
- ZNF598 specifically functions in poxvirus infection of cell lines lacking ISG responses
- Poxvirus protein synthesis requires ZNF598 ubiquitin ligase activity
- Poxvirus replication requires ubiquitination of the ZNF598 substrate, RPS20

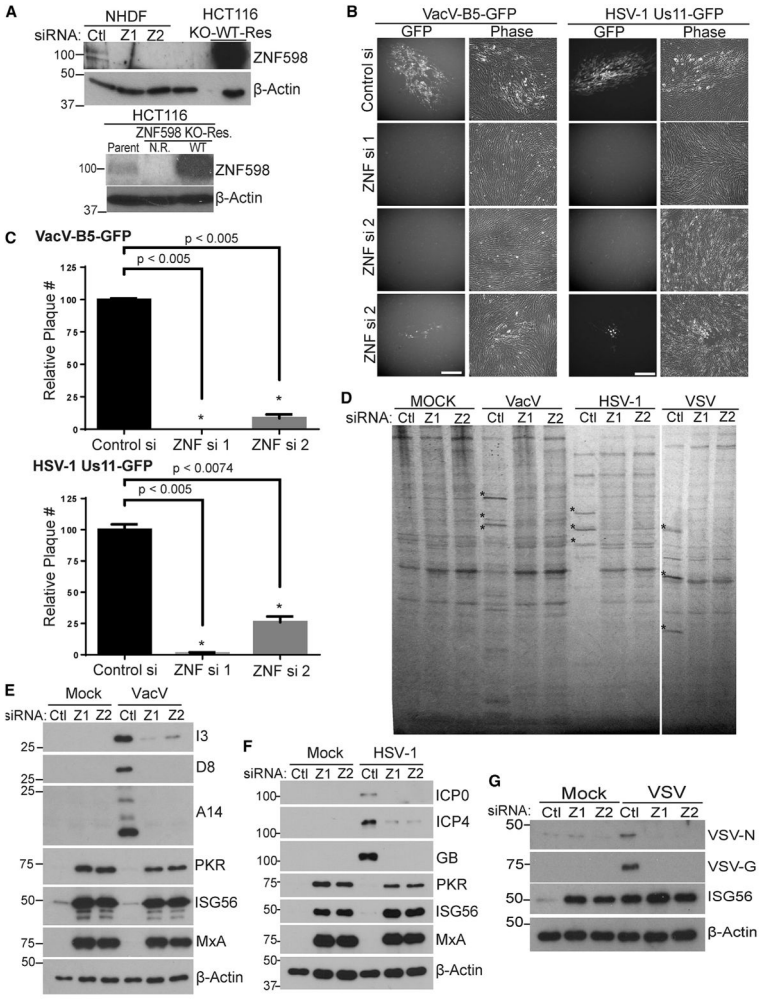

Figure 1. Depletion of ZNF598 Induces a Broad Antiviral State in Primary Human Cells

NHDFs were treated with control (ctrl) non-targeting siRNAs or independent siRNAs targeting ZNF598 (Z1, Z2).

(A) Upper: WB validation of siRNA-mediated ZNF598 depletion in NHDFs. Unlabeled lane is a repeat load of siRNA-treated sample. As a control and reference for ZNF598 detection and abundance, lysates from HCT116 ZNF598-KO cells rescued with WT ZNF598 were included. Lower: lanes 1–3 of Figure 2C, showing the migration of ZNF598 as a doublet and its relatively low-level expression in HCT116 parental cells compared against ZNF598-KO cells rescued with WT ZNF598. N.R., no rescue. Greater doublet resolution in NHDFs reflects longer gel running time.

(B) Cultures were infected with VacV-B5-GFP or HSV-1-Us11-GFP at MOI 0.003 for 2 days to allow spread. Representative phase and fluorescence images are shown. Where detected for Z2-treated cultures plaques were smaller than controls. Bar, 300 μm.

(C) Quantification of plaque numbers in (B), presented relative to controls as mean ± SEM n = 3; unpaired two-tailed t test.

(D) Cultures were infected at MOI 5 with VacV (20 hr), HSV-1 (20 hr), or VSV (4 hr; accounting for its fast replication cycle) followed by ^{35}SMet/Cys labeling. Asterisks

highlight examples of viral proteins in control samples, whose synthesis is suppressed by ZNF598 depletion.

(E–G) siRNA-treated NHDFs were infected with different viruses as indicated. Samples were analyzed by WB with the indicated antibodies. Molecular weight markers in kilodaltons are to the left.

(E) Cultures infected with VacV at MOI 5 for 20 hr.

(F) Cultures infected with HSV-1 at MOI 5 for 20 hr.

(G) Cultures infected with VSV at MOI 5 for 4 hr. Note that VSV infection induced ISG56 expression even in control siRNA-treated cells, illustrating normal antiviral responses in primary NHDFs. $n \geq 3$ biological replicates for all experiments.

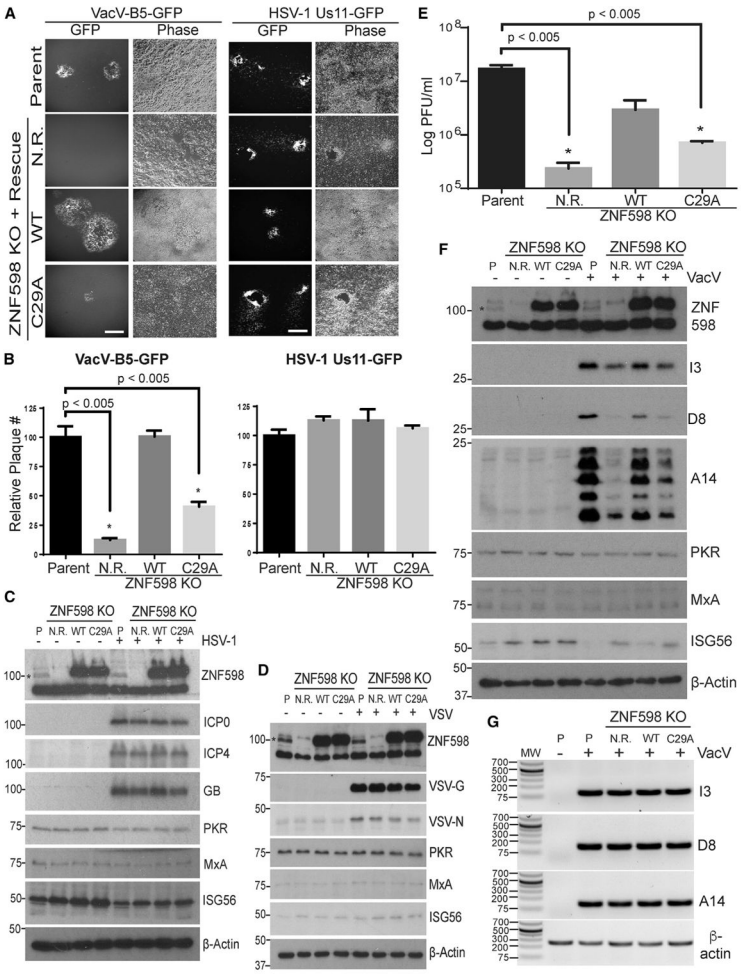

Figure 2. ZNF598 Ubiquitin Ligase Activity Is Specifically Required for Poxvirus Protein Synthesis

Parental (P) HCT116 cells alongside HCT116 ZNF598 knockout (KO) cells that were not rescued (N.R.) or rescued with wild-type (WT) or ubiquitin ligase mutant (C29A) forms of ZNF598.

(A) Cells were infected with VacV-B5-GFP or HSV-1-Us11-GFP at MOI 0.003 for 2 days to form plaques. Representative phase and fluorescence images are shown. While reduced in number, even when detectable in C29A rescue cells VacV plaques were smaller than controls. Bar, 300 μm.

(B) Quantification of plaque numbers in (A), presented relative to controls as mean ± SEM n = 3; unpaired two-tailed t test.

(C–F) HCT116 cells were infected with different viruses as indicated. Samples were analyzed by WB with the indicated antibodies. Asterisks highlight ZNF598. Molecular weight markers in kilodaltons are to the left.

(C) Cells infected with HSV-1 at MOI 5 for 20 hr.

(D) Cells infected with VSV at MOI 5 for 4 hr.

(E and F) Cells infected with VacV at MOI 10 for 20 hr.

(E) Levels of infectious virus produced in each cell line. Data are presented as mean ± SEM n = 3; unpaired two-tailed t test.

(F) WB analysis of VacV and ISG protein levels.

(G) Cultures were infected with VacV at MOI 10 for 20 hr. RNA was isolated and analyzed by reverse transcriptase PCR for the indicated mRNAs. Molecular weight markers in bp are indicated. n ≥ 3 biological replicates for all experiments.

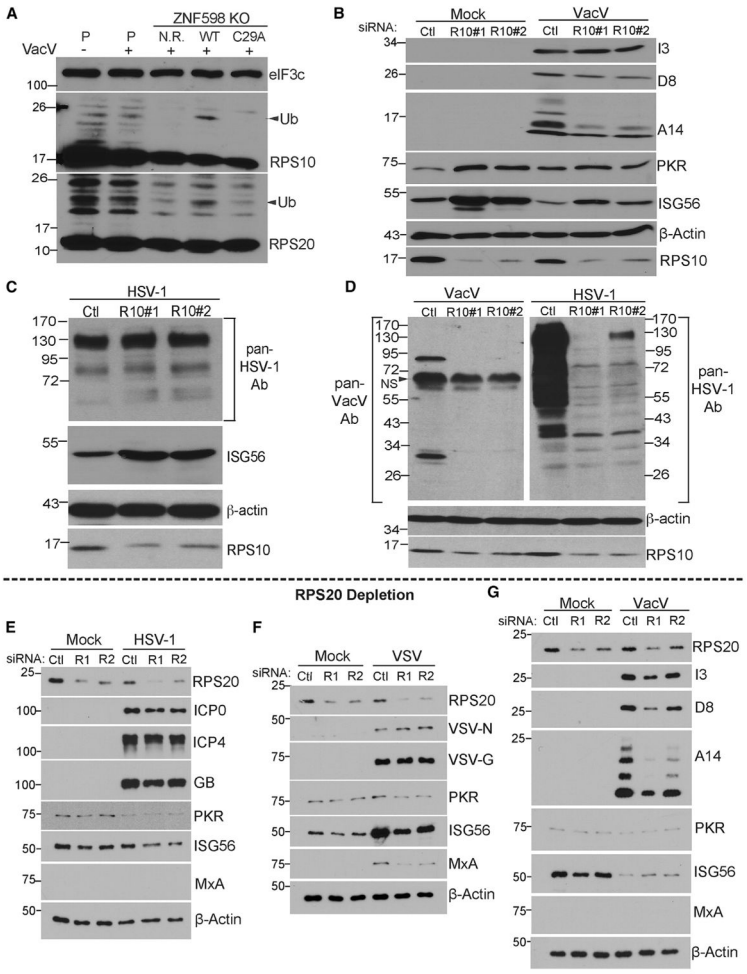

Figure 3. Differential Roles for RPS Substrates of ZNF598 during Infection in Primary Human Cells

(A) HCT parental (P) alongside ZNF598-KO cells that were not rescued (N.R.) or rescued with WT or ubiquitin ligase mutant (C29A) forms of ZNF598 were infected with VacV at MOI 10 for 20 hr. Samples were analyzed by WB using the indicated antibodies. ZNF598-responsive ubiquitinated (Ub) forms of RPS10 and RPS20 are highlighted. n = 2.

(B–D) NHDFs were treated with control (Ctrl) non-targeting siRNAs or independent siRNAs targeting RPS10 (R10#1, R10#2). Cells were infected as indicated and samples were analyzed by WB. Pan-HSV-1 or Pan-VacV antibodies raised against virus particles detect multiple structural proteins. Non-specific (NS) bands detected with these pan-antibodies are highlighted. Molecular weight markers in kilodalton are indicated.

(B) Cells infected with VacV at MOI 5 for 20 hr.

(C) Cells infected with HSV-1 at MOI 5 for 20 hr.

(D) Cells infected with VacV or HSV-1 at MOI 0.001 for 3 days to allow virus spread.

(E–G) NHDFs were treated with control non-targeting siRNAs or independent siRNAs targeting RPS20 (R1, R2). Cells were infected as indicated and samples were analyzed by WB. Molecular weight markers in kilodaltons are indicated.

(E) Cells infected with HSV-1 at MOI 5 for 20 hr.

(F) Cultures infected with VSV at MOI 5 for 4 hr.
(G) Cells infected with VacV at MOI 5 for 20 hr. n ≥ 3 biological replicates unless otherwise indicated.

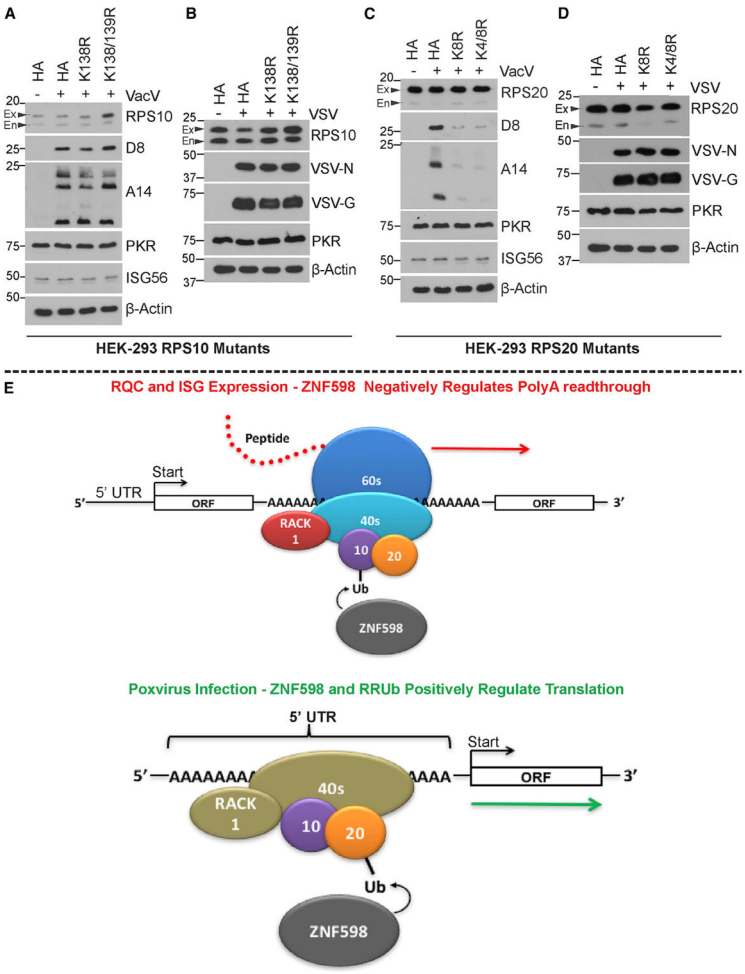

Figure 4. RPS20 Ubiquitination Specifically Affects Poxvirus Infection

(A and B) HEK293 cells expressing RPS10 WT or lysine-arginine mutants K138R or K138/139R were infected with VacV or VSV. Samples were analyzed by WB with the indicated antibodies. Arrows highlight exogenous (Ex) and endogenous (En) forms of RPS10. Molecular weight markers in kilodaltons are indicated.

(A) VacV infection at MOI 0.001 for 3 days.

(B) VSV infection at MOI 0.001 for 1 day (approximating to the same number of replication cycles as VacV in A).

(C and D) HEK293 cells expressing RPS20 WT or lysine-arginine mutants, K8R or K4/8R were infected and processed as for RPS10 lines above. Arrows highlight exogenous (Ex) and endogenous (En) forms of RPS20.

(C) VacV infection at MOI 0.003 for 3 days.

(D) VSV infection at MOI 0.003 for 1 days. n = 3 biological replicates.

(E) A model for ZNF598 and regulatory ribosome ubiquitination (RRUb) in host versus poxvirus translation. Host context (top): ZNF598 and RRUbs are involved in stalling of decoding 80S ribosomes on long poly(A) tracts that repress translation (red arrow) and induce RQC. Shorter poly(A) sequences ≥11 nt that induce ribosome sliding are present in codons of KIR genes, nucleotide binding proteins, and transcriptional regulators and may

also be subject to readthrough repression by ZNF598 to control ISG expression. ZNF598-mediated repression of RQC and ISG expression appears to be more dependent on RPS10 than RPS20 (see main text). Poxvirus context (bottom): Poxviruses cause several unique modifications to RPSs (represented as change in 40S color) and have poly(A) tracts in their 5′ UTRs rather than in coding regions. ZNF598 and RPS20 ubiquitination stimulate poxvirus translation (green arrow), suggesting additional roles for ZNF598 and RRUb in scanning.